18th Australasian Fluid Mechanics Conference
Launceston, Australia
3-7 December 2012

Comparison of Wind Turbine actuator methods using Large Eddy Simulation

J. E. Cater[1], S. E. Norris[2] and R C.Storey[1]

[1]Department of Engineering Science
University of Auckland, Auckland 1142, New Zealand

[2]Department of Mechanical Engineering
University of Auckland, Auckland 1142, New Zealand

Abstract

This work presents a comparison between a range of actuator models for Horizontal Axis Wind Turbines (HAWT). Large Eddy Simulation (LES) and an aero-elastic turbine simulation were coupled to model turbines. This coupling results in a transient turbine wake and a model that permits the simulation of real-time control directives and wake interaction. The FAST aero-elastic code and a research LES code were selected for this study. Coupling of the codes was implemented using a partitioned software framework capable of parallelised operation on distributed computing resources. Actuator models can impose restrictive conditions on the simulation time-stepping algorithm, which increases the computational cost. In this work, comparisons of three types of turbine model were conducted for a non-dimensional model of a HAWT.

Introduction

Sørensen and colleagues [1, 2] introduced the actuator disc method with finite difference approximations to the Euler equations for numerical modelling of wind turbines. This technique was further developed by Mikkelsen [3] and Ivanell [4] and applied to the Reynolds averaged Navier-Stokes (RANS) equations. In the actuator disc method, the turbine blade forces are averaged azimuthally over the rotor area to give a radially varying load distribution. This method has been shown to agree with one dimensional momentum theory, however limitations have been identified when results are compared to field measurements. Differences in the flow field are a result of the assumption that the blade forces are dependent only on radial position and can be averaged for span-wise sections in the azimuthal direction. In typical operating conditions, vertical shear in the atmospheric boundary layer causes a variation of blade loading with elevation; horizontal shear due to yawed flow can also cause variation in blade loading across the rotor span.

Sørensen and Shen [5] developed the actuator line model to address these limitations by representing individual blades as lines, onto which aerodynamic forces are projected. This method captures the vorticity being shed from the blade tips and the diametric variation of blade forces associated with horizontal or vertical wind shear. An advantage of the actuator line model is its ability to model blade-scale turbulence generated at the rotor and in the turbine wake, however this increase in resolution comes at a significant computational cost. The majority of the additional processing is associated with the restriction placed on the time-step of transient methods such as LES. For numerical stability reasons similar to those associated with a Courant-Friedrich-Levy (*CFL*) number condition, the displacement of the actuator line tip is limited to the transit of a single computational mesh cell per time-step. Thus, for flows where the actuator line tip speed is higher than the maximum flow speed, this condition specifies the upper limit for the time-step interval.

In the present work, a hybrid actuator model, the 'Actuator Sector Method', has been developed where the resolution offered by the actuator line technique is retained while the computational expense associated with the small time-steps required for stability is reduced. This is achieved through a temporal distribution of aerodynamic forces, based on the simulation time-step, over a sector region swept by a representative line during that interval. Results from the actuator sector model are compared to the actuator disc and actuator line techniques.

Numerical Methodology

Flow Solver

The computations presented in this work were conducted using a custom CFD code called SnS. This code was developed at the Universities of Auckland and Sydney a [6, 7]. The code models transient flows using a structured, non-staggered mesh using a fractional step solver [8].

For wind turbine modelling, turbine forces can be prescribed, or calculated during the simulation using FAST, a BEM based aero-elastic code developed at NREL [9]. In this instance, the FAST code operates in a coupled simulation with SnS where information on the flow field at the turbine and the resulting aerodynamic response are shared during the simulation; this is explained in more detail in a previous publication [10]. Turbine forces are interpolated onto the computational mesh according to the specified turbine model. A modified differencing scheme was used in a volume around the turbine by implementing a flux limiter to the second order scheme [11]. This technique was selected to introduce minimal local diffusion in a restricted region. More extensive validation of the tools used in this work has been conducted in a previous paper [12], where wake simulations were compared to theoretical and measured field data showing acceptable results.

Actuator Modelling

In the conventional actuator disc method, a circular surface, representing the turbine rotor, is mapped onto the computational mesh. The forces on the flow due to the action of the turbine, f_i, can be averaged over annular rings within the disc to represent radial variation in load, or averaged over the entire disc. The total thrust on the rotor is given by equation 1 where f_i is the force on the flow as a function of radius, R is the radius of the rotor and θ is the azimuthal direction.

$$T_{disc} = -\int_0^{2\pi}\int_0^R f_i(r)\,\mathrm{d}r\mathrm{d}\theta \tag{1}$$

In the actuator line model, forces are consolidated onto line elements representing the turbine blades. The total thrust on the rotor is given in equation 2, where B is the number of blades. The consolidation of aerodynamic forces onto a discrete moving line gives rise to a revised numerical stability condition.

$$T_{line} = -\sum_{b=1}^{B} \int_0^R f_{i,b}(r)\,\mathrm{d}r \tag{2}$$

Numerical Stability

For a general time-advancing numerical scheme, a *CFL* number less than unity is often required for accuracy (and possibly stability). This condition is shown in equation 3, where u_i^{max} is the maximum flow velocity in the i^{th} direction, Δt is the time step, and Δx_i^{min} is the minimum mesh spacing in the i^{th} direction.

$$CFL = \frac{u_i^{max}\Delta t}{\Delta x_i^{min}} < 1 \tag{3}$$

In the case of the actuator disc, the stability of a time-advancing simulation is dependent on the standard *CFL* number. For an actuator line model, where the line velocity is greater than u_i^{max} a new stability criteria is imposed. This is defined in equation 4 such that the value of CFL_{line} must also be less than unity. For the case of an actuator line model of a HAWT, the maximum line velocity is given by ωR, where ω is the rotational velocity of the rotor in radians per second, and R is the rotor radius. Assuming that the mesh spacing is equal in all directions, the ratio between the two *CFL* conditions is given by $\omega R/u_i^{max}$.

$$CFL_{line} = \frac{u_i^{max}\Delta t}{\Delta x_i^{min}} = \frac{\omega R \Delta t}{\Delta x_i^{min}} < 1 \tag{4}$$

A parameter commonly defined in turbine modelling is the tip speed ratio (TSR), λ, defined in equation 5, where u_{ref} is the upstream reference wind speed at the turbine hub height.

$$\lambda = \frac{\omega R}{u_{ref}} \tag{5}$$

This relation can be modified by instead referring to u_i^{max}. Using the modified TSR, λ^*, the range of operating conditions for which the CFL_{line} condition is in effect is defined for $\lambda^* > 1$.

$$\lambda^* = \frac{\omega R}{u_i^{max}} \tag{6}$$

In practice, the *CFL* number is generally restricted to a nominal value less than unity, depending on the flow conditions and solution scheme. For $CFL = 0.5$ the CFL_{line} condition would then be in effect for $\lambda^* > 2$. For typical wind turbine simulations, u_i^{max} can conservatively be estimated to be no more than $1.5u_{ref}$. A variety of flow conditions can produce u_i^{max} including large fluctuations in the atmospheric boundary layer (ABL) or speed up around the perimeter of the turbine due to the velocity deficit in the wake of the rotor where the flow diverges. With this estimate, the CFL_{line} stability condition is effective for $\lambda > 3$. For modern wind turbines, a majority of operating time would be spent at higher TSRs ($\lambda > 4$).

The Actuator Sector Method

In this new model, the Actuator Sector Method, aerodynamic forces acting on the flow are integrated in the time domain. Instead of a single line being mapped onto the mesh, multiple lines are introduced over the sector range, each with a portion of the equivalent line force. The force distribution along the line is either prescribed during the simulation, or calculated prior to the force distribution algorithms; this occurs for each blade individually. This results in the distribution of forces onto sectors representing the area swept by the turbine blade during each time-step of the numerical scheme. The total thrust on the rotor is given in equation 7, where ϕ represents the angle through which a representative line has travelled during a time-step Δt.

$$T_{sector} = -\sum_{b=1}^{B} \int_0^{\phi} \int_0^R f_{i,b}(r)\,\mathrm{d}r\mathrm{d}\theta \tag{7}$$

The time-step of the simulation is reliant only on a standard *CFL* condition as the actuator sector can transit multiple computational cells without introducing discontinuities of force in the azimuthal plane. The angle ϕ is given by: $\phi = \Delta\theta = \omega\Delta t$. Such that the start of the sector is defined by the azimuth position of the blade at the start of the time step, and the end of the sector, by the position at the end of the time step. Forces are then distributed uniformly over the sector area with respect to the azimuthal direction, to represent the time-integrated contribution of the forces on the fluid. A representation of the three actuator methods is shown in figure 1 demonstrating the effective azimuthal extent of the actuator models.

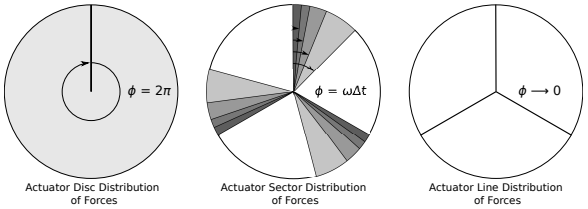

Figure 1: The distribution of aerodynamic forces at the turbine rotor plane for the actuator disc model (left) the Actuator Sector Method (centre) and the actuator line model (right).

In figure 2, the initial sample line is placed at the previous azimuth position of the blade, θ_1 (evaluated at t_1), with equidistant samples used up to the current azimuth position, θ_2 (evaluated at $t_2 = t_1 + \Delta t$). The number of line samples is proportional to the ratio of the sector angle to the computational mesh spacing. Along each sample line, a set of equidistant points are sampled, at which the aerodynamic forces are calculated using cubic spline interpolation. The number of sample points along a line is also proportional to the mesh spacing. At each sample point, each of the three components of force are tri-linearly distributed in Euclidean space to the eight surrounding mesh cell centres. This is illustrated in figure 2 in two-dimensions, where the linear weightings of the force at each point are given by α_i and β_i. There is a constant sampling of points along the sample line (not each cell).

An investigation into both sector line sampling and line point sampling showed that the integral of forces applied has a maximum error of less than 0.5% when 10 sample points and 5 lines are used per mesh cell. Following the evaluation of turbine forces at mesh cell centres, a filter is applied to remove discontinuities in the rotor plane. The filtering function was based on a technique developed for an actuator line where the filtering width was scaled by the computational mesh spacing. In the Actuator Sector implementation, this function was re-parameterised to be scaled by the actuator sector angle. This function spreads forces in the direction normal to the rotor plane, and azimuthally, both leading and trailing the blade position. This technique does not spread forces in the radial direction beyond the rotor region, as this has been shown to affect power output calculations. The filter width is scaled to the Actuator Sector angle to ensure the rate of change of force at a

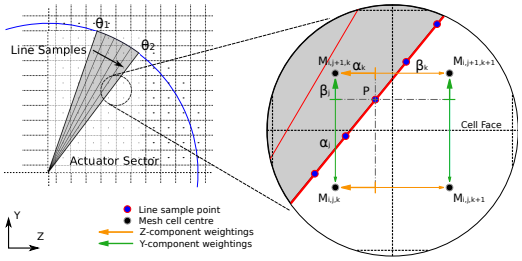

Figure 2: A distribution of aerodynamic forces onto a two-dimensional computational mesh for the Actuator Sector Method. The thick red line represents the equivalent of an actuator line, and in this case is the final sample line for the Actuator Sector method.

point on the rotor is kept constant for a varying sector angle. This ensures the flow accelerations at the rotor are consistent with a actuator line model using the same filtering technique. The filtering function is based on the convolution of the force distribution with a box kernel in the azimuthal direction.

A box kernel gives a linear weighting function. The kernel width can be varied by a parameter (σ) specifying the ratio of filter width to sector angle. For the following computations this was set at two.

Non-Dimensional Turbine Results

Simulations were conducted for an idealised, non-dimensionalised turbine operating in uniform laminar flow. The turbine structure was assumed to be rigid and the aerodynamic effects of the tower and nacelle are omitted. Both axial and rotational aerodynamic forces are included in the turbine model to fully describe the turbine response. A 3-bladed turbine was modelled using a unit rotor radius, density and reference velocity with $\lambda = 7$. A constant normal and tangential induction was prescribed across the turbine with an axial induction factor of $\alpha = 0.3$. The associated Reynolds number based on rotor diameter was set to 200 by adjusting the fluid viscosity. The turbine blades were divided into equidistant elements for which the blade loading was evaluated. The constant axial and tangential induction gave a linearly increasing load distribution with respect to radial position. A Prandtl tip loss model was included to avoid a load discontinuity at the blade tip.

Flow Domain

The extent of the flow domain was determined based on the turbine radius and the computational mesh was refined around the turbine as shown in figure 3. The schematic illustrates a constant mesh spacing in the turbine region; outside of this region the mesh expands exponentially to the boundaries in the Y and Z directions. The cell size in the refined region was set to 50 cells per rotor diameter, with a total of 11.25×10^6 cells in the entire domain. At the inlet, a uniform laminar flow was prescribed and a zero pressure condition enforced at the outlet. Periodic conditions were applied to the remaining boundaries. These dimensions give a blockage ratio of $\pi/100$ for this turbine model in the simulation domain.

Model Comparisons

Simulations were conducted for the actuator disc, actuator line and two Actuator Sector models under identical flow conditions. The simulation parameters for the non-dimensionalised cases are summarised in table 1. The simulation time was based on a large eddy turn-over time (LETOT) given by L/u_{ref}, where L is the smallest cross stream dimension of the flow domain. For the

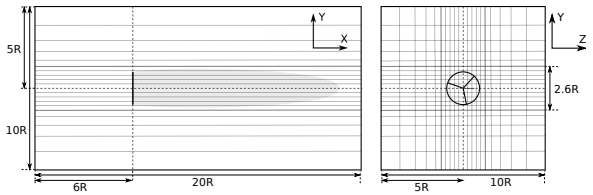

Figure 3: The flow domain for the non-dimensional turbine simulations, showing mesh refinement around the turbine and a representative wake. The mesh spacing in the X-direction is constant.

prescribed flow conditions, a simulation duration of 20 LETOTs was executed. Time-averaged results were calculated over the final half of the simulation duration. C_T is the thrust coefficient given by equation 8. A is the swept area of the turbine rotor.

$$C_T = \frac{T}{\frac{1}{2}\rho u_{ref}^2 A} \tag{8}$$

Table 1: Simulation Time-step Parameters

	CFL Range	Mean *CFL*	$\Delta t u_{ref}/R$
Disc	0.4 - 0.5	0.410	0.0016
Sector, Case 1	0.4 - 0.5	0.430	0.0016
Sector, Case 2	0.25 - 0.35	0.271	0.0010
Line	-	0.135	0.0005

The flow domains for each case were analysed by comparing integrals of important flow quantities and turbine thrust coefficient. The total thrust applied by the model was calculated for each case to verify the force distribution algorithms. The average velocity at the turbine from the time-averaged results was recorded as well as the total simulation CPU times. These data are presented in table 2.

Table 2: Performance Comparison

	C_T	u_{ave}/u_{ref}	Relative CPU
Disc	0.802	0.760	0.333
Sector, Case 1	0.803	0.759	0.295
Sector, Case 2	0.803	0.760	0.536
Line	0.802	0.758	1.000

For a prescribed thrust coefficient of 0.806, the maximum error in the thrust coefficient for all methods is less than 0.5%. The average velocity evaluated at the rotor was over-predicted with a maximum error of 8.4%. This can be explained by a combination of the blockage effect and the tip-loss correction. The total processing durations are significantly reduced for the Actuator Sector Method cases when compared to the actuator line model. A 70% reduction in CPU time is achieved when comparing Actuator Sector Case 1 and the actuator line. The calculation time for Actuator Sector Case 1 is in fact lower than for the actuator disc due to the reduced convergence times for the flow pressure solver.

Instantaneous results are presented in figure 4 and figure 5 where contours of velocity and vorticity magnitude, Ω, have been evaluated at the rotor plane. The sector angle in Actuator Sector Case 1 was calculated at 0.112 rad and decreases to 0.07 rad in Case 2. This corresponds to a transit of 2.8 cells at the blade tip for Case 1 and 1.8 cells for Case 2. Significant difference in the velocity and vorticity fields are shown between the actuator disc and the Actuator Sector Method in figures 4 and

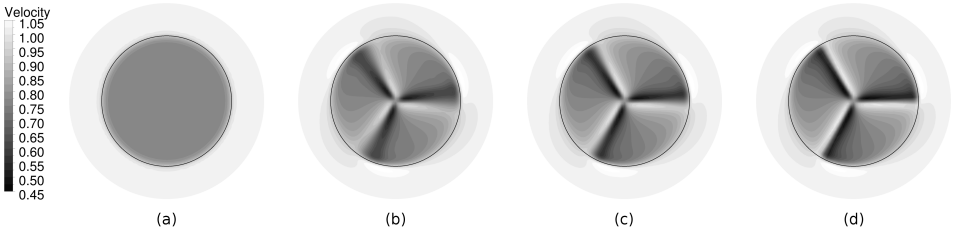

Figure 4: Instantaneous contours of non-dimensionalised velocity (u/u_{ref}) at the rotor plane for (a) the Actuator Disc, (b) Actuator Sector Case 1, (c) Actuator Sector Case 2 and (d) the Actuator Lines. The rotor plane perimeter is indicated by the thick black ring.

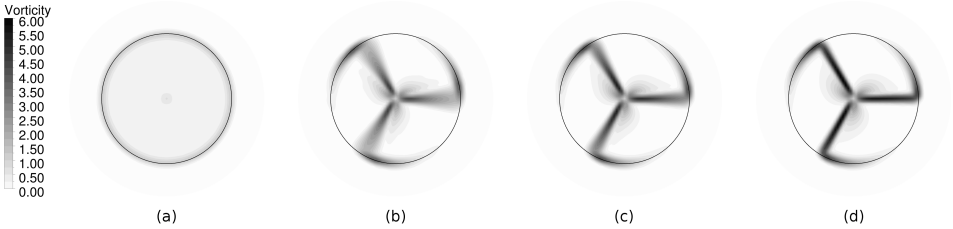

Figure 5: Instantaneous contours of non-dimensionalised vorticity magnitude ($\Omega R/u_{ref}$) at the rotor plane for (a) the Actuator Disc, (b) Actuator Sector Case 1, (c) Actuator Sector Case 2 and (d) the Actuator Lines. The rotor plane perimeter is indicated by the thick black ring.

5. Plots (b) through (d) show the effect of the varying sector angle on the vorticity field, where the velocity gradients at the blade are reduced for increased sector angles. These variations are also seen in the accompanying velocity plots. Overall, a significant increase in spatial resolution of the flow variations is achieved compared to the actuator disc method.

Conclusions

The Actuator Sector model thus offers a viable alternative to transient flow simulations employing conventional actuator disc models, with minimum additional computational cost. This is especially significant in sheared flows such as in an atmospheric boundary layer or in yawed flow where the actuator line has shown improved agreement with measured data when compared to actuator disc models.

Acknowledgments

The authors would like to acknowledge the funding of a University of Auckland Doctoral Scholarship and the support of the Faculty of Engineering at The University of Auckland through a Faculty Research Development Fund grant. The contributions to the CFD code by S. Armfield from The University of Sydney are greatly appreciated.

References

[1] J. N. Sørensen and A. Myken. Unsteady actuator disc model for horizontal axis wind turbines. *Journal of Wind Engineering and Industrial Aerodynamics*, 39(13):139 – 149, 1992.

[2] J. N. Sørensen, W. Z. Shen, and X. Munduate. Analysis of wake states by a full-field actuator disc model. *Wind Energy*, 1(2):73–88, 1998.

[3] R. Mikkelsen. *Actuator Disk Methods Applied to Wind Turbines*. PhD thesis, Technical University of Denmark, 2003.

[4] S. Ivanell. *Numerical Computations of Wind Turbine Wakes*. PhD thesis, Gotland University, 2009.

[5] J.N. Sorensen and W.Z. Shen. Numerical modeling of wind turbine wakes. *Journal of Fluids Engineering - Transactions of the ASME*, 124(2):393–399, 2002.

[6] S. W. Armfield, S. E. Norris, P. Morgan, and R. Street. A parallel non-staggered Navier-Stokes solver implemented on a workstation cluster. In *Computational Fluid Dynamics 2002: ICCFD2*, pages 30–45, 2003.

[7] S. E. Norris. *A Parallel Navier–Stokes Solver for Natural Convection and Free Surface Flow*. PhD thesis, University of Sydney, 2000.

[8] S. W. Armfield and R. Street. An analysis and comparison of the time accuracy of fractional-step methods for the Navier-Stokes equations on staggered grids. *International Journal for Numerical Methods in Fluids*, 38:255–282, 2002.

[9] J. M. Jonkman and M. L. Buhl Jr. FAST User's Guide. Technical report, National Renewable Energy Laboratory, 2005.

[10] R. C. Storey, S. E. Norris, K. A. Stol, and J. E. Cater. Large eddy simulation of dynamically controlled wind turbines in an offshore environment. *Journal of Wind Energy*, 1(1):1, 2012.

[11] B. P. Leonard and S. Mokhtari. Beyond first-order upwinding: The ULTRA-SHARP alternative for non-oscillatory steady-state simulation of convection. *Journal of Numerical Methods in Engineering*, 30:729–766, 1990.

[12] R. C. Storey, S. E. Norris, , K. A. Stol, and J. E. Cater. Large eddy simulation of dynamically controlled wind turbines using actuator discs. In *Proceedings of the 30th Wind Energy Symposium*. AIAA, Jan 2011.